Received 9 January 2006
Revised 22 April 2006
Accepted 6 September 2006

Developing mixed convection of a nanofluid in a horizontal tube with uniform heat flux

M. Akbari and A. Behzadmehr
Mechanical Engineering Department, University of Sistan and Baluchistan, Zahedan, Iran

Abstract

Purpose – This paper seeks to show the effect of using nanofluid on mixed convection heat transfer in a horizontal tube.

Design/methodology/approach – Three-dimensional elliptic governing equation has been solved using finite volume approach. Grid independence test has been performed to find the suitable grids. Obtained numerical results have been validated with the available experimental and numerical results in the literature. Parametric study has been done to see the effects of Reynolds number, Grashof number and volume fraction of the nanoparticles on the hydrodynamic and thermal parameters in a horizontal tube.

Findings – The nanoparticles volume fraction does not have a direct effect on the secondary flow and the skin friction coefficient. However, its effect on the entire fluid temperature causes the strength of the secondary flow to reduce. For a given Grashof number, increasing the particles' concentration augments convective heat transfer coefficient. It does not have a significant effect on the skin friction coefficient at the low Grashof number. However, skin friction coefficient is slightly affected at the higher Grashof numbers.

Research limitations/implications – The Grashof number is limited for which the Boussinesq hypothesis for the variation of density with the temperature would be valid.

Practical implications – This paper promotes designing heat exchangers, solar collectors, cooling electronic devices.

Originality/value – Nanofluid mixed convection in a horizontal tube has been studied and the effects of nanoparticles concentration on the hydrodynamic and thermal parameters have been shown and discussed.

Keywords Heat transfer, Convection, Boiler tubes

Paper type Research paper

Nomenclature

C_B = Boltzmann constant (1.38×10^{-23} J/K)
C_f = Peripherally average skin friction coefficient
C_p = Specific heat (J/kg K)
D = Tube diameter (m)
D_s = nanoparticle diameter (m)
g = Gravitational acceleration (m/s^2)
Gr = Grashof number $((= g\beta_{eff} q_w D^4)/(k_{eff}\upsilon_{eff}^2))$
h = Convection heat transfer coefficient (Wm^2 K)
k = Thermal conductivity (W/m K)
Nu_m = Peripherally average Nusselt number
P = Pressure (pa)
Pe = Peclet number $(= 3\pi D_s^3 D(-(dP/dZ))/(4C_B T))$
q_w = Uniform heat flux (W/m^2)
r = Radial direction

International Journal of Numerical Methods for Heat & Fluid Flow
Vol. 17 No. 6, 2007
pp. 566-586

0961-5539
DOI 10.1108/09615530710761216

The authors thank University of Sistan and Baluchistan for its support. Comments of the unknown reviewers are also gratefully acknowledged.

Re = Reynolds number ($= \rho_{eff} w_0 D/\mu_{eff}$)
T = Temperature (K)
u = Tangential velocity component (m/s^1)
v = Radial velocity component (m/s^1)
w = Axial velocity component (m/s^1)
Z = Axial direction

Greek letters
α = Thermal diffusivity (m^2/s^1)
β = Volumetric expansion coefficient (1/K)
θ = Angular coordinate
Φ = Volume fraction
μ = Dynamic viscosity (N s/m^2)
ν = Kinematic viscosity (m^2/s^1)
ρ = Density (kg/m^3)

Subscripts
b = Bulk
eff = Effective
f = Base fluid
m = Average
D = Inlet condition
s = solid particles
w = Wall

Introduction

Low thermal conductivity of conventional heat transfer fluids such as water, oil, and ethylene glycol mixture is a serious limitation in improving the performance and compactness of many engineering equipments such as heat exchangers and electronic devices. To overcome this disadvantage, there is strong motivation to develop advanced heat transfer fluids with substantially higher conductivity. An innovative way of improving the thermal conductivities of fluids is to suspend small solid particles in the fluid. However, more than a century ago Maxwell (1873, 1904) showed the possibility of increasing thermal conductivity of a mixture by more volume fraction of solid particles.

Various types of powders such as metallic, non-metallic and polymeric particles can be added into fluids to form slurries. An industrial application test was carried out by Liu *et al.* (1988) and the effects of flow rates on the slurry pressure drop and heat transfer behavior was investigated. In conventional cases the suspended particles are of μm or even mm dimensions. However, such large particles may cause severe problems such as abrasion and clogging. Therefore, fluids with suspended large particles have little practical application in heat transfer enhancement.

Nanofluids are a new kind of heat transfer fluid containing a small quantity of nano-sized particles (usually less than 100 nm) that are uniformly and stably suspended in a liquid. The dispersion of a small amount of solid nanoparticles in conventional fluids changes their thermal conductivity remarkably. Compared to the existing techniques for enhancing heat transfer, the nanofluids show a superior potential for increasing heat transfer rates in a variety of cases. Choi (1995) quantitatively analyzed some potential benefits of nanofluids for augmenting heat transfer and reducing size, weight and cost of thermal apparatuses, while incurring little or no penalty in the pressure drop.

Researchers have demonstrated that oxide ceramic nanofluids consisting of CuO or Al_2O_3 nanoparticles in water or ethylene glycol exhibit enhanced thermal conductivity (Lee *et al.*, 1999). A maximum increase in thermal conductivity of approximately 20 per cent was observed in that study, having 4 per cent vol. CuO nanoparticles with mean diameter 35 nm dispersed in ethylene glycol. A similar behavior has been observed in Al_2O_3/water nanofluid. For example, using Al_2O_3 particles having a mean diameter of 13 nm at 4.3 per cent volume fraction increased the thermal conductivity of water under stationary conditions by 30 per cent (Masuda *et al.*, 1993).

On the other hand, larger particles with an average diameter of 40 nm led to an increase of less than 10 per cent (Lee *et al.*, 1999). Furthermore, the effective thermal conductivity of metallic nanofluid increased by up to 40 per cent for the nanofluid consisting of ethylene glycol containing approximately 0.3 per cent vol. Cu nanoparticles of mean diameter less than 10 nm (Choi, 1995).

Different concepts have been proposed to explain this enhancement in heat transfer. Xuan and Li (2000) and Xuan and Roetzel (2000) have identified two causes of improved heat transfer by nanofluids: the increased thermal dispersion due to the chaotic movement of nanoparticles that accelerates energy exchanges in the fluid and the enhanced thermal conductivity of nanofluids considered by Choi (1995). On the other hand, Kelbinski *et al.* (2002) have studied four possible mechanisms that contribute to the increase in nanofluid heat transfer: Brownian motion of the particles, molecular-level layering of the liquid/particle interface, heat transport in the nanoparticles and nanoparticles clustering. Similarly to Wang *et al.* (1999), they showed that the effects of the interface layering of liquid molecules and nanoparticles clustering could provide paths for rapid heat transfer. Numerous theoretical and experimental studies have been conducted to determine the effective thermal conductivity of nanofluids. Most of these have been confined to liquids containing micro- and milli-sized suspended solid particles. However, studies show that the measured thermal conductivity of nanofluids is much larger than the theoretical predictions (Choi *et al.*, 2001). Many attempts have been made to formulate efficient theoretical models for the prediction of the effective thermal conductivity, but there is still a serious lack in this domain (Xue, 2003, Xuan *et al.*, 2004).

As nanofluids are rather new, relatively few theoretical and experimental studies have been reported on convective heat transfer coefficients in confined flows. Pak and Cho (1998) and Xuan and Li (2000, 2003) obtained experimental results on convective heat transfer for laminar and turbulent flow of a nanofluid inside a tube. They produced the first empirical correlations for the Nusselt number using nanofluids composed of water and Cu, TiO_2 and Al_2O_3 nanoparticles. The results indicate a remarkable increase in heat transfer performance over the base fluid for the same Reynolds number.

Despite the fact that nanofluid is a two phase mixture, since the solid particles are very small size they are easily fluidized and can be approximately considered to behave as a fluid (Xuan and Li, 2000). Therefore, considering the ultrafine and low-volume fraction of the solid particles, it might be reasonable to treat nanofluid as single phase flow in certain conditions (Yang *et al.*, 2005).

The single-phase approach assumes that the fluid phase and particles are in thermal equilibrium and move with the same velocity. This approach is simpler and requires less computational time. Thus, it has been used in several theoretical studies of convective heat transfer with nanofluids (Maiga *et al.*, 2004; Roy *et al.*, 2004; Khanafer *et al.*, 2003; Koo and Kleinstreuer, 2005). However, due to the fact that the effective properties of nanofluids are not known precisely, the numerical predictions of this approach are; in general, depend on the considered effective physical properties.

Mixed convection in horizontal tubes at the macro-level which appears in many industrial installations has been studied extensively (Mori *et al.*, 1966; Petukhov *et al.*, 1969; Patankar *et al.*, 1978; Siegwarth and Hanratty, 1970; Cheng and Yuen, 1985; Ciampi *et al.*, 1986; Zhang, 1992; Hwang and Lai, 1994). At such conditions, a secondary

flow pattern could be created because of buoyancy force which significantly enhances heat transfer. It is well known, that the buoyancy force and adding naoparticles in a fluid trends to increase heat transfer. However, the interaction of these both effects has not been studied.

The objective of the present paper is to study the effects of particles concentration on the hydrodynamic and thermal parameters of developing laminar mixed convection of a nanofluid in a horizontal tube at different *Re* and *Gr*. Simultaneous effect of buoyancy force and adding nanoparticles in the fluid, on heat transfer augmentation are studied. Therefore, the axial velocity, secondary flow and temperature profiles for different values of the particles concentration are presented at different axial positions. Also, the axial evolution of the convective heat transfer coefficient and the skin friction coefficient are shown and discussed.

Mathematical formulation and numerical procedure

Mixed convection of a nanofluid consists of water and Al_2O_3 in a long horizontal tube ($D = 0.02$ m and $Z = 1.96$ m) with uniform heat flux at the solid-liquid interface has been considered. Figure 1 shows the geometry of the considered problem. Gravitational force is exerted in the vertical direction. Therefore, symmetry is considered about the vertical central plane and the calculations have been done on one-half of the cylinder. The properties of the fluid are assumed constant except for the density in the body force, which varies linearly with the temperature (Boussinesq's hypothesis). Dissipation and pressure work are neglected. In order to be able using single phase approach, altrafine (< 100 nm) solid particles is considered. Owing to their non sedimenting nature, behaves as single phase fluid for which the fluid phase and nanoparticles are in thermal equilibrium with zero relative velocity (Xuan and Roetzel, 2000; Putra *et al.*, 2003; Daungthongsuk and Wongwises, 2007). With these assumptions the dimensional conservation equations for steady state mean conditions are as follows.

Continuity equation

$$\frac{1}{r}\frac{\partial}{\partial\theta}(\rho_{\text{eff}}u) + \frac{1}{r}\frac{\partial}{\partial r}(\rho_{\text{eff}}rv) + \frac{\partial}{\partial Z}(\rho_{\text{eff}}w) = 0 \tag{1}$$

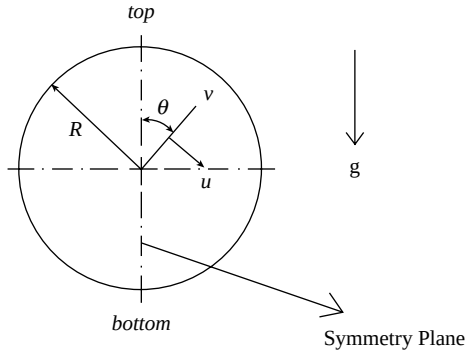

Figure 1.
Schematic of the horizontal tube cross section

Momentum equation

$\theta -$ component:

$$\frac{1}{r}\frac{\partial}{\partial\theta}(\rho_{\text{eff}}uu)+\frac{1}{r}\frac{\partial}{\partial r}(\rho_{\text{eff}}rvu)+\frac{\partial}{\partial Z}(\rho_{\text{eff}}wu)+\frac{1}{r}(\rho_{\text{eff}}uv)$$
$$=-\frac{1}{r}\frac{\partial p}{\partial\theta}+\frac{1}{r^2}\frac{\partial}{\partial\theta}\left(\mu_{\text{eff}}\frac{\partial u}{\partial\theta}\right)+\frac{\partial}{\partial r}\left(\frac{\mu_{\text{eff}}}{r}\frac{\partial(ru)}{\partial r}\right)+\frac{2\mu_{\text{eff}}}{r^2}\frac{\partial v}{\partial\theta} \tag{2a}$$
$$+\rho_{\text{eff}}g\beta_{\text{eff}}(T_{\text{w}}-T)\sin\theta$$

$r -$ component:

$$\frac{1}{r}\frac{\partial}{\partial\theta}(\rho_{\text{eff}}uv)+\frac{1}{r}\frac{\partial}{\partial r}(\rho_{\text{eff}}rvv)+\frac{\partial}{\partial Z}(\rho_{\text{eff}}wv)-\frac{1}{r}\rho_{\text{eff}}u^2$$
$$=-\frac{1}{r}\frac{\partial p}{\partial r}+\frac{1}{r^2}\frac{\partial}{\partial\theta}\left(\mu_{\text{eff}}\frac{\partial v}{\partial\theta}\right)+\frac{\partial}{\partial r}\left(\frac{\mu_{\text{eff}}}{r}\frac{\partial(rv)}{\partial r}\right)-\frac{2\mu_{\text{eff}}}{r^2}\frac{\partial u}{\partial\theta} \tag{2b}$$
$$-\rho_{\text{eff}}g\beta_{\text{eff}}(T_{\text{w}}-T)\cos\theta$$

$Z -$ component:

$$\frac{1}{r}\frac{\partial}{\partial\theta}(\rho_{\text{eff}}uw)+\frac{1}{r}\frac{\partial}{\partial r}(\rho_{\text{eff}}rvw)+\frac{\partial}{\partial Z}(\rho_{\text{eff}}ww)$$
$$=-\frac{\partial p}{\partial Z}+\frac{1}{r^2}\frac{\partial}{\partial\theta}\left(\mu_{\text{eff}}\frac{\partial w}{\partial\theta}\right)+\frac{1}{r}\frac{\partial}{\partial r}\left(r\mu_{\text{eff}}\frac{\partial w}{\partial r}\right) \tag{2c}$$

Energy equation

$$\frac{1}{r}\frac{\partial}{\partial\theta}(\rho_{\text{eff}}uT)+\frac{1}{r}\frac{\partial}{\partial r}(\rho_{\text{eff}}rvT)+\frac{\partial}{\partial z}(\rho_{\text{eff}}wT)$$
$$=\frac{1}{r^2}\frac{\partial}{\partial\theta}\left(\frac{K_{\text{eff}}}{(C_p)_{\text{eff}}}\frac{\partial T}{\partial\theta}\right)+\frac{\partial}{r\partial r}\left(r\frac{K_{\text{eff}}}{(C_p)_{\text{eff}}}\frac{\partial T}{\partial r}\right) \tag{3}$$

The properties of nanofluid (fluid containing suspended nanoparticles) are defined as follows:

Density

$$\rho_{\text{eff}}=(1-\phi)\rho_{\text{f}}+\phi\rho_{\text{s}} \tag{4}$$

where indices f and s corresponded to the based fluid and nanoparticle, respectively.

Effective thermal conductivity

$$k_{\text{eff}}=\left[\frac{k_{\text{s}}+(n-1)k_{\text{f}}-(n-1)\phi(k_{\text{f}}-k_{\text{s}})}{k_{\text{s}}+(n-1)k_{\text{f}}+\phi(k_{\text{s}}-k_{\text{f}})}\right]k_{\text{f}} \tag{5}$$

This was introduced by Hamilton and Crosser (1962). Where n is a shape factor and considers equal to 3 for spherical nanoparticles:

Thermal diffusivity

$$\alpha_{\text{eff}}=\frac{k_{\text{eff}}}{(1-\phi)(\rho C_p)_{\text{f}}+\phi(\rho C_p)_{\text{s}}} \tag{6}$$

Thermal expansion coefficient

$$\beta_{\text{eff}} = \left[\frac{1}{1+((1-\phi)\rho_{\text{f}})/\phi\rho_{\text{s}})}\ \frac{\beta_{\text{s}}}{\beta_{\text{f}}} + \frac{1}{1+(\phi/(1-\phi))(\rho_{\text{s}}/\rho_{\text{f}})}\right]\beta_{\text{f}} \tag{7}$$

This was used by Khanafer *et al.* (2003).

Specific heat

$$(Cp_{\text{eff}}) = \left[\frac{(1-\phi)(\rho C_p)_{\text{f}} + \phi(\rho C_p)}{(1-\phi)\rho_{\text{f}} + \phi\rho_{\text{s}}}\right] \tag{8}$$

Effective viscosity of water – Al_2O_3 nanofluid:

$$\mu_{\text{eff}} = (123\phi^2 + 7.3\phi + 1)\mu_{\text{f}} \tag{9}$$

which was presented by Maiga *et al.* (2004) for water – Al_2O_3 nanofluid based on available experimental results in the literature.

The boundary conditions are as follows:

- At the tube inlet ($Z = 0$):

$$w = w_0, \quad u = v = 0, \quad T = T_0 \tag{10}$$

- At the fluid-solid interface ($r = D/2$):

$$w = u = v = 0 \text{ and } q_{\text{w}} = -k_{\text{eff}}\frac{\partial T}{\partial r} \tag{11}$$

- At vertical symmetry plane:

$$\theta = 0 \text{ and } \theta = \pi, \quad u = 0, \quad \frac{\partial v}{\partial \theta} = \frac{\partial w}{\partial \theta} = \frac{\partial T}{\partial \theta} = 0 \tag{12}$$

At the tube outlet ($Z/D = 98$) the diffusion flux in the direction normal to the exit plane is assumed to be zero for all variables and an overall mass balance correction is applied.

This set of coupled nonlinear differential equations was discretized with the control volume technique. For the convective and diffusive terms a second order upwind method was used while the SIMPLEC procedure was introduced for the velocity-pressure coupling. The discretization grid is uniform in the circumferential direction and non-uniform in the other two directions. It is finer near the tube entrance and near the wall where the velocity and temperature gradients are large.

Validation and results

In this section we show results calculated with the previously presented model, which demonstrate its versatility and illustrate the effect of particles concentration on the flow field at different *Gr* and *Re*.

Validation

Several different grid distributions have been tested to ensure that the calculated results are grid independent. The selected grid for the present calculations consisted of 180, 40 and 20 nodes, respectively, in the axial, radial and circumferential directions. As it shows in Figure 2(a) and 2(b), increasing the grid numbers does not significantly change

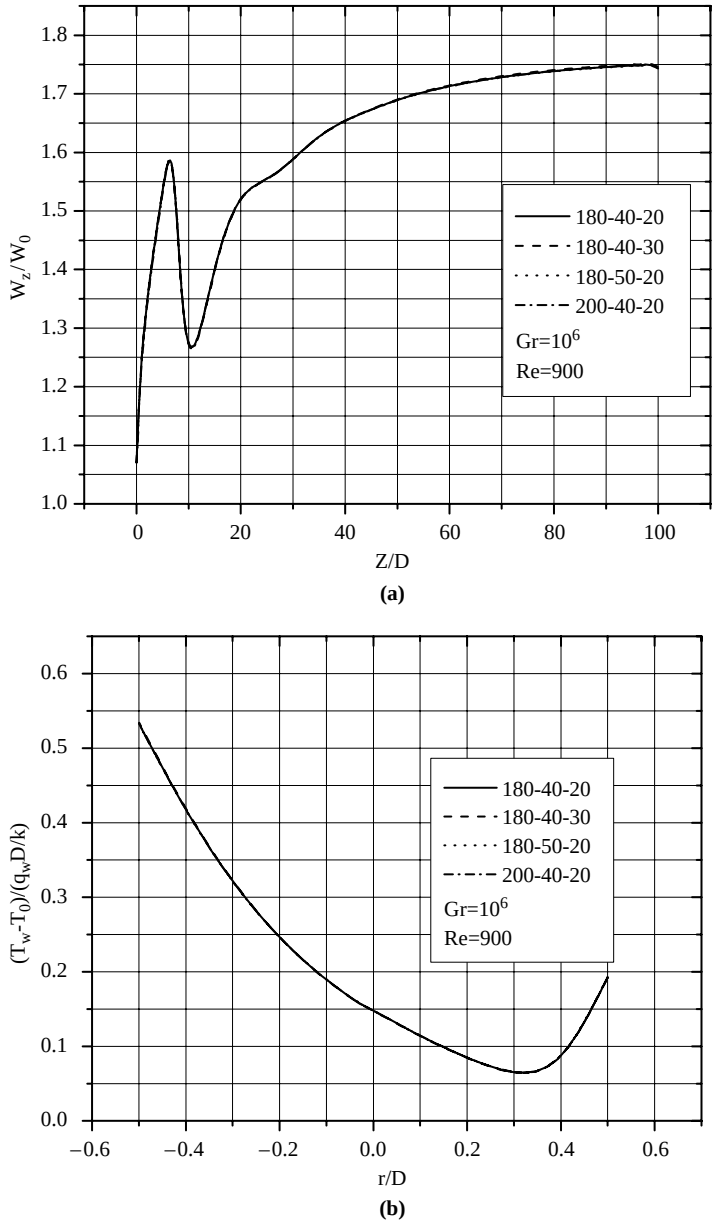

Figure 2.
Grid independence tests (a) dimensionless centerline axial velocity profile along the tube length; (b) dimensionless temperature variation at the fully developed region

centerline axial velocity along the tube length and temperature at the radial direction at fully developed region. Other axial and radial profiles are also verified to be sure the results are grid independence. However, because of limited space they are not presented.

In order to demonstrate the validity and also precision of the model and the numerical procedure, calculated velocity and temperature profiles have been compared with corresponding experimental and numerical results available in the literature.

Figure 3 shows the comparison of the calculated results with Barozzi *et al.* (1998) experimental results in a horizontal tube. As it is shown, the axial evolution of mixed convection Nusselt number is in good agreement with the corresponding experimental results. Another comparison has also been performed with the numerical results obtained by Choudhury and Patankar (1988). Comparison of the fully developed axial velocity profile is shown in Figure 4(a). The concordance between these results is also good. Figure 4(b) compares the dimensionless temperature along the tube length. Again the results are in good agreement. Therefore, the numerical procedure is reliable and can predict developing mixed convection flow in a horizontal tube.

Results

Numerical simulations have been done on a wide range of *Re* and *Gr* for five different values of particles concentrations. However, because of similar behavior and also lake of space the results presented here are for $Re = 300$ and two *Gr* (low and high Grashof numbers) with three different values of particles concentrations (0, 2, 4 per cent). Maximum Grashof number (or wall heat flux) at each Reynolds number are limited by

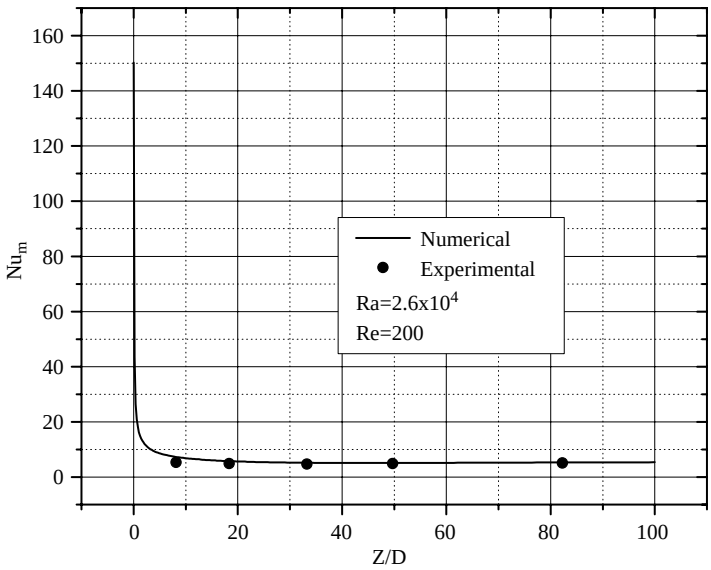

Figure 3.
Comparison of axial evolution of the peripheral average *Nu* with the Barozzi *et al.* (1998) experimental results

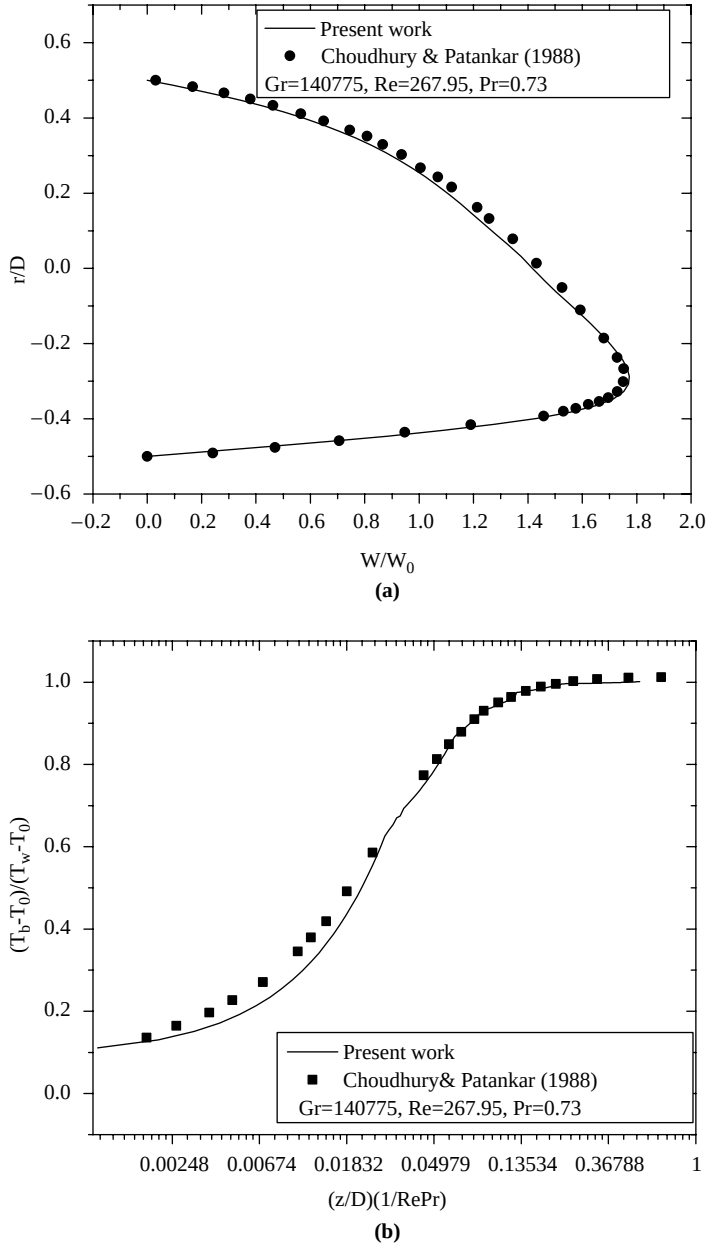

Figure 4.
Comparison with Choudhury and Patankar (1988) numerical results (a) fully developed axial velocity; (b) axial evolution of dimensionless temperature

the value of increasing bulk temperature. This value respected the suggested criteria for validation of the Boussinesq approximation which was presented by Nesreddine *et al.* (1997).

Also, these conditions respected the situations were experimentally presented by Ding and Wen (2005) for which particles distribution could be considered uniform in the fluid (very small Peclet number). Peclet number (*Pe*) in the present conditions is less than 0.006.

For a given *Re* and three different values of the Al_2O_3 particles concentrations (0, 2 and 4 per cent vol.), vectors of dimensionless secondary flow ($uD/\alpha,\ vD/\alpha$) and also contours of dimensionless temperature ($(T - T_0/(q_w D/k_{eff})$) at different cross sections along the tube length are presented for two different Grashof numbers ($Gr = 5 \times 10^4,\ Gr = 7 \times 10^5$). Figure 5 shows these vectors and contours at $Z/D = 10$. The fluid rises along the heated wall up to top of the tube and falls down slowly toward the centre because of buoyancy force. Therefore, a secondary flow pattern appears at the tube cross section which creates a circular cell. Its position depends on the buoyancy force and the inertia of the secondary flow at the vertical plane (symmetry plane). At the tube entrance, the centre of cell establishes in the upper portion of the tube. At $Z/D = 10$ contour of temperature is fairly circular for the low *Gr* because of low value of heat which transfers to the fluid at this position. However, increasing the Grashof number ($Gr = 7 \times 10^5$) augments the buoyancy force and consequently stronger secondary flow appears. The latter causes the centre of recirculation moves downward and close to the tube wall. Such a strong secondary flow distorted the contours of temperature at the upper part of the tube while they still are in circular shape at the lower part of the tube where the secondary flow is weak. The effects of particles concentration are also shown in this Figure. Adding 2 per cent Vol. Al_2O_3 nanoparticles in water increases the effective conductivity of the fluid, so the molecular heat diffusion augments. Therefore, for a given *Gr* and *Re* fluid temperature becomes more uniform by increasing particle concentrations. While the secondary flow, despite of higher heat flux needs to keep the Grashof number constant for higher particles concentration, does not change significantly.

Figures 6-8 shows these vectors and contours at different axial positions along the tube length. By moving downstream, the secondary flow becomes weaker while the centre of the circulation cell moves downward and approaches to the tube wall. At the tube entrance, boundary layer is not developed and the wall heating energy could not easily transfer entire the tube cross section. Therefore, the gradient of temperature at the near wall region becomes significant while temperature at the centre region does not significantly affect. Further downstream, boundary layer grows and develops along the tube length while the fluid flow temperature rises. Increasing fluid temperature at the centerline region augments the buoyancy force at this region. This force is in opposite direction of the secondary flow's inertia which comes from top of the tube towards the centerline region. Thus, by moving along the tube length the strength of the secondary flow decreases. The variation of the temperature at different cross sections is shown in Figure 9. At $Z/D = 10$ the centre line region is fairly constant and is in minimum value. However, further downstream centerline temperature increases and its minimum value appears far

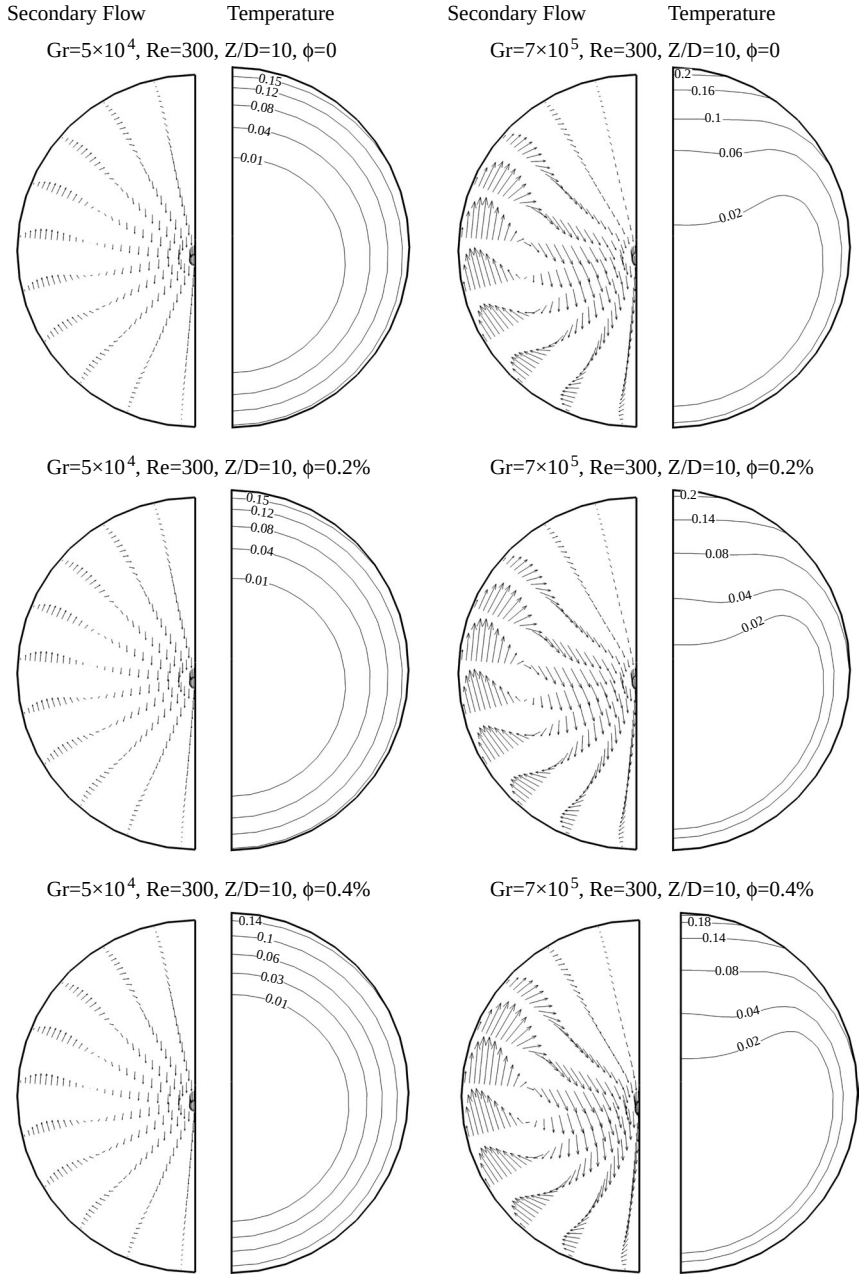

Figure 5.
Dimensionless vectors of secondary flow and contours of temperature at $Z/D = 10$

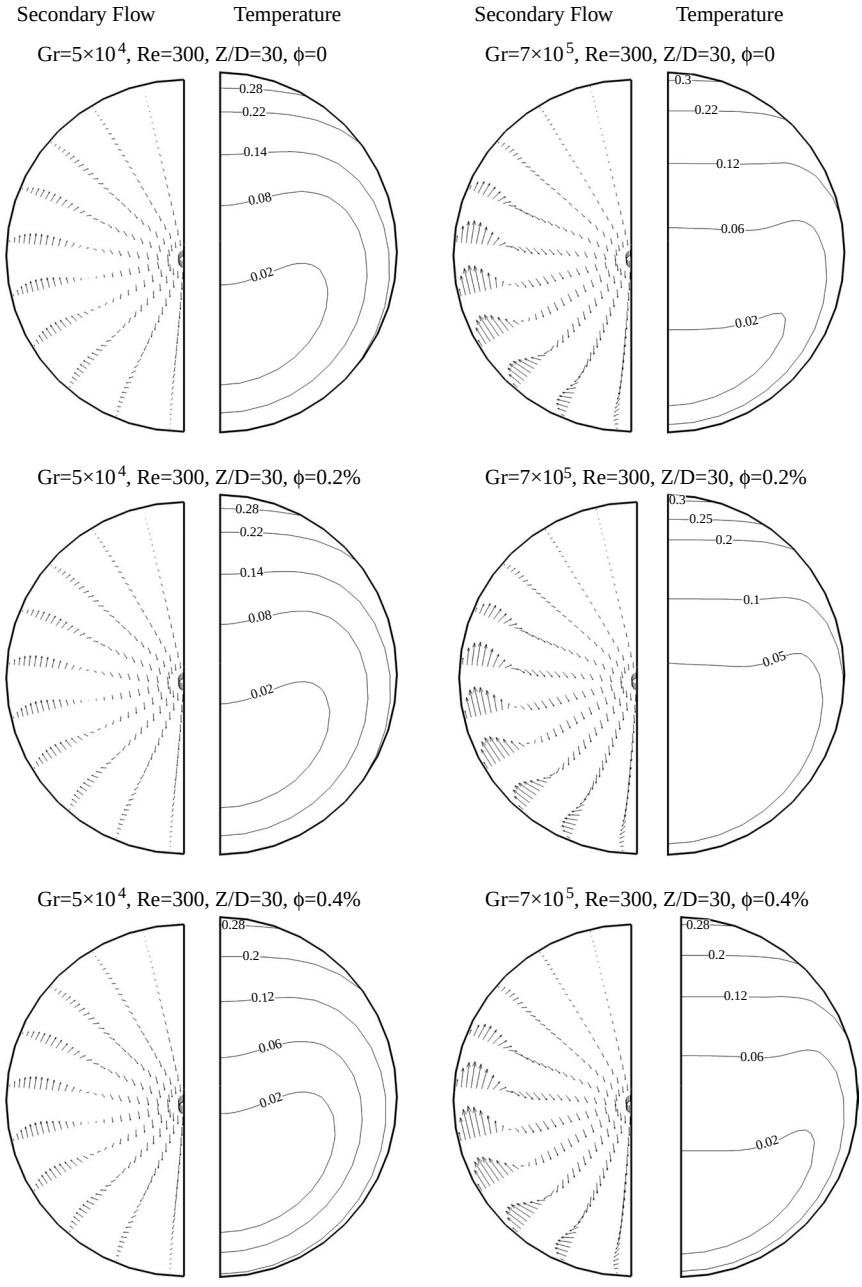

Figure 6.
Dimensionless vectors of secondary flow and contours of temperature at $Z/D = 30$

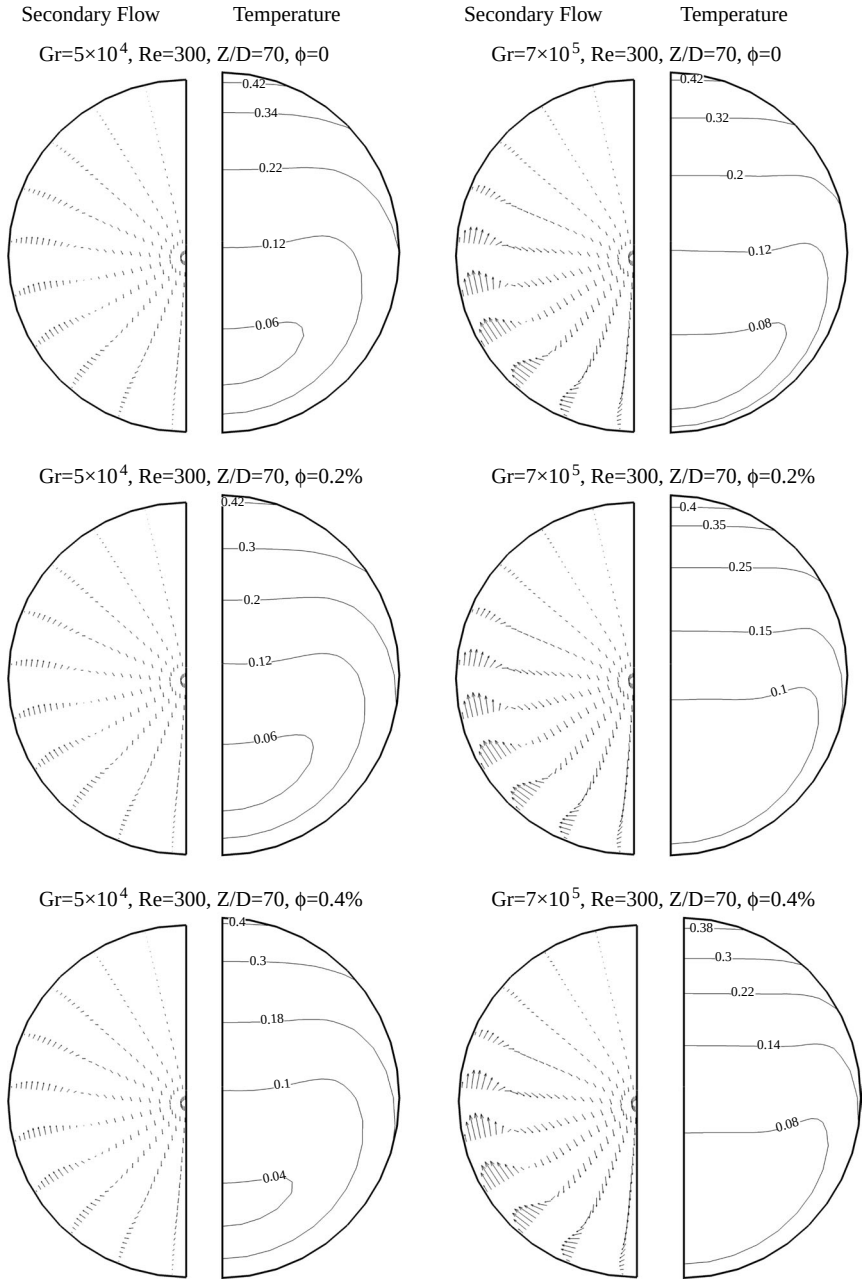

Figure 7.
Dimensionless vectors of secondary flow and contours of temperature at $Z/D = 70$

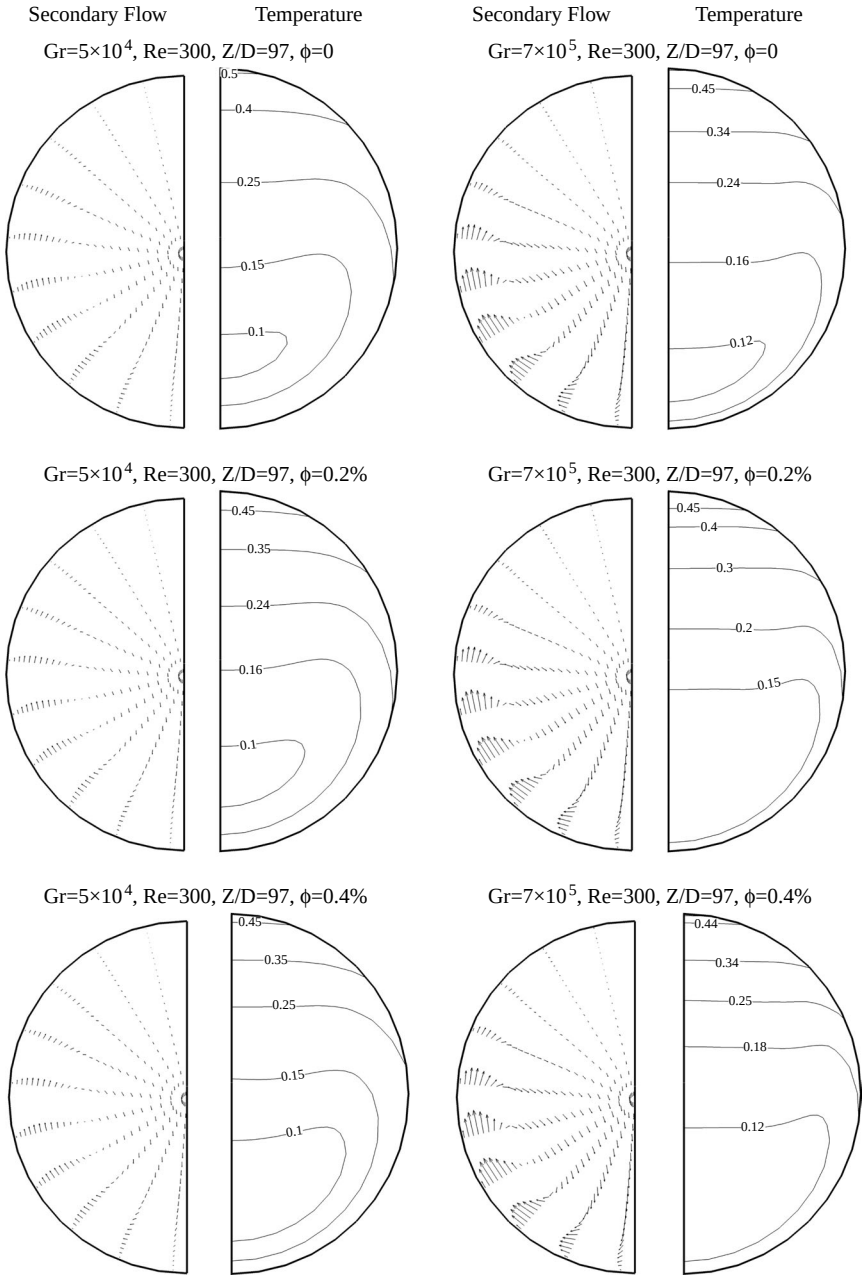

Figure 8.
Dimensionless vectors of secondary flow and contours of temperature at $Z/D = 97$

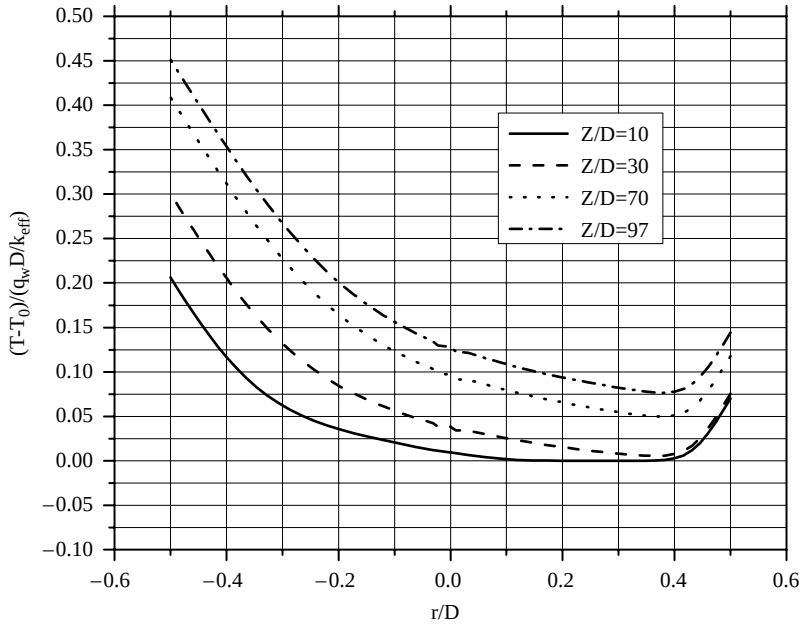

Figure 9.
Dimensionless temperature on the vertical plane at different axial positions

from the centerline and approaches to the bottom tube wall. This explains why the circulation cell in the secondary flow displaces to the bottom portion.

Figure 10 shows the axial velocity profiles at four different cross sections for a given *Re* at $Gr = 5 \times 10^4$ and $Gr = 7 \times 10^5$. Secondary flow distorted the axial velocity profile and so the maximum velocity no longer appears at the centerline. At the low Grashof number, moving downstream the velocity profile is more distorted and its maximum value displaces toward the bottom tube wall. The asymmetric axial velocity profiles at the fully developed region ($Z/D = 70$ or $Z/D = 97$) are most pronounced. Where, the buoyancy effect is the strongest. At higher Grashof number, velocity profile becomes more asymmetric. However, contrary to the lower Grashof number, velocity profile is less distorted at higher *Z/D*.

Effect of particles concentration on the axial velocity profiles is shown in Figure 11. As it is clearly seen, the particles concentration does not have significant effect on the axial velocity profiles. Figure 12 shows the axial evolution of the convective heat transfer coefficient. It decreases and goes to its fully developed value monotonically. The effect of nanoparticles concentration on h is positive and increases the heat transfer coefficient. However, the rate of increasing heat transfer coefficient decreases by using nanofluid consisting of higher nanoparticles concentration. The same behavior is also seen at the higher Grashof number. Convective heat transfer coefficient increases 9 per cent by adding 2 per cent Vol. Al_2O_3 nanoparticles. While its value augments 15 per cent by adding 4 per cent Vol. Al_2O_3 nanoparticles.

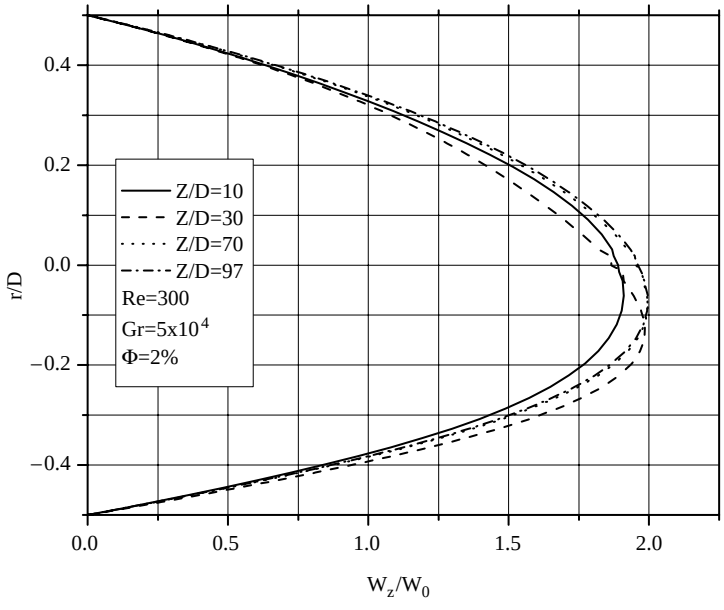

(a)

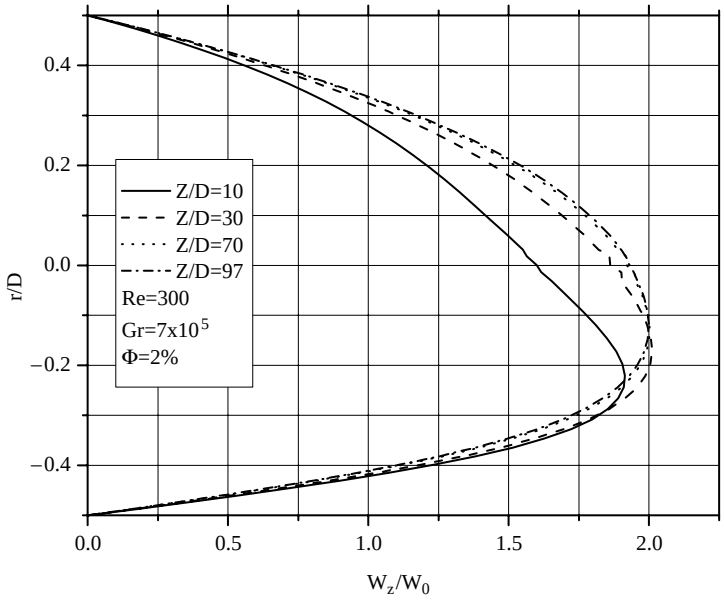

(b)

Figure 10.
Dimensionless axial velocity profiles at different axial positions (a) $Gr = 5 \times 10^4$; (b) $Gr = 7 \times 10^5$

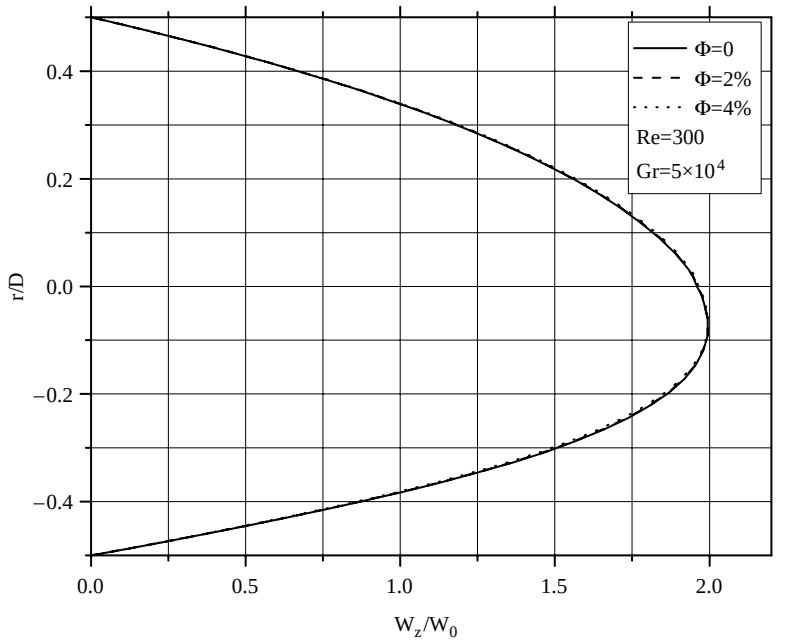

Figure 11.
Effect of nanoparicles concentrations on the fully developed axial velocity

Axial evolution of the skin friction is shown in Figure 13. As it is shown increasing the nanoparticles concentration does not change the skin friction at the low Grashof numbers. The same behavior was also experimentally shown by Xuan and Li (2003) in the case of forced convection in a circular tube (negligible buoyancy force). However, by increasing the Grashof numbers for which the buoyancy force augments, the nanoparticles concentration could reduce the skin friction coefficient.

Conclusion

Developing laminar mixed convection of a nanofluid consists of water and Al_2O_3 in a horizontal tube has been studied numerically. The results illustrate that the nanoparticles concentration does not have significant effect on the secondary flow pattern and the axial velocity. The fluid temperature is affected directly because of increasing the thermal molecular diffusion. Increasing the nanoparticles concentration augments significantly the convective heat transfer coefficient. For a given Grashof number, as the buoyancy force at the centerline region of the tube increases, the secondary flow pattern becomes weaker. This is reduces the heat transfer coefficient. In addition, augmentation of the particles concentration tends to uniform the entire fluid temperature. These effects are affected the skin friction coefficient for which at the high value of the Grashof number, increasing the nanoparticles concentration could reduce the skin friction coefficient. While at the low *Gr*, it does not have significant effect on the skin friction coefficient.

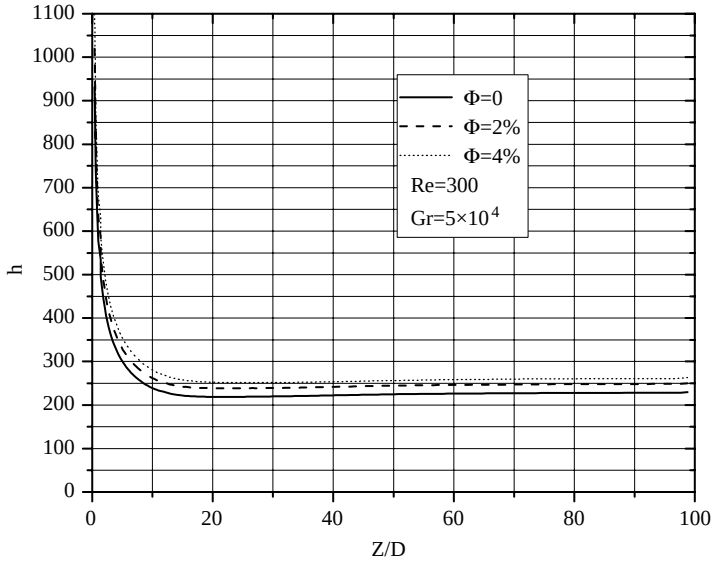

(a)

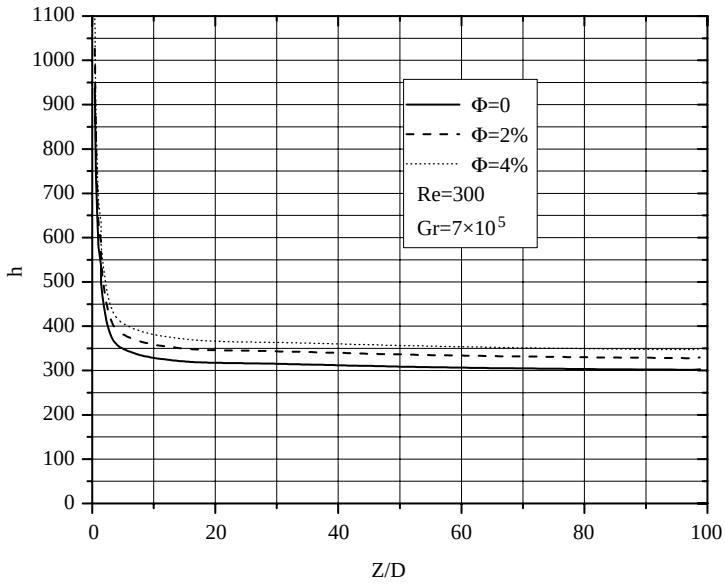

(b)

Figure 12.
Axial evolution of the peripheral average convective heat transfer coefficient for different values of the particles concentrations
(a) $Gr = 5 \times 10^4$;
(b) $Gr = 7 \times 10^5$

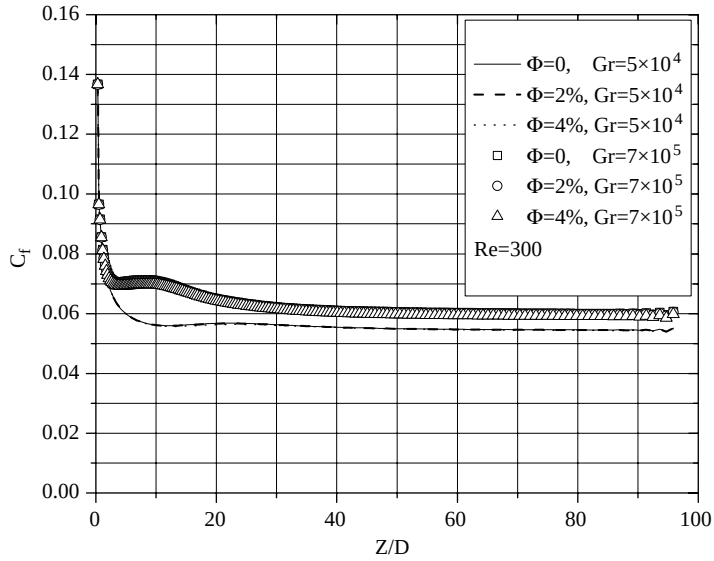

Figure 13.
Axial evolution of the peripheral average skin friction coefficient for different values of the particles concentrations (a) $Gr = 5 \times 10^4$; (b) $Gr = 7 \times 10^5$

References

Barozzi, G.S., Zanchini, E. and Mariotti, M. (1998), "Experimental investigation of combined forced and free convection in horizontal and inclined tubes", *Meccanica*, Vol. 20, pp. 18-27.

Cheng, K.C. and Yuen, F.P. (1985), "Flow visualization studies on secondary flow pattern for mixed convection in the thermal entrance region of isothermally heated inclined pipes ASME", *Heat Transfer Division*, Vol. 42, pp. 121-30.

Choi, S.U.S. (1995), "Enhancing thermal conductivity of fluid with nanoparticles, developments and applications of non-Newtonian flow", *ASME*, FED 231/MD 66, pp. 99-105.

Choi, S.U.S., Zhang, Z.G., Yu, W., Lockwood, F.E. and Grulke, E.A. (2001), "Anomalous thermal conductivity enhancement in nanotube suspensions", *Applied Physics Letters*, Vol. 79 No. 14, pp. 2252-4.

Choudhury, D. and Patankar, S.V. (1988), "Combined forced and free laminar convection in the entrance region of an inclined isothermal tube", *J. Heat Transfer Trans. ASME*, Vol. 110 No. 4, pp. 901-9.

Ciampi, M., Faggiani, S., Grassi, W., Incropera, F.P. and Tuoni, G. (1986), "Experimental study of mixed convection in horizontal annuli for low Reynolds numbers", *Proceedings of the International Heat Transfer Conference*,Vol. 3, pp. 1413-8.

Daungthongsuk, W. and Wongwises, S. (2007), "A critical review of convective heat transfer of nanofluids", *Renewable and Sustainable Energy Reviews*, Vol. 11 No. 5, pp. 797-817.

Ding, Y. and Wen, D. (2005), "Particle migration in a flow of nanoparticle suspensions", *Powder Technology*, Vol. 149, pp. 84-92.

Hamilton, R.L. and Crosser, O.K. (1962), "Thermal conductivity of heterogeneous two-component system", *I & EC Fundamentals*, Vol. 1 No. 3, pp. 187-91.

Hwang, G.J. and Lai, H.C. (1994), "Laminar convection heat transfer in a horizontal isothermal tube for high Reynolds numbers", *Int. J. Heat Mass Transfer*, Vol. 37 No. 11, pp. 1631-40.

Keblinski, P., Phillpot, S.R., Choi, S.U.S. and Eastman, J.A. (2002), "Mechanisms of heat flow in suspensions of nano-sized particles (nanofluid)", *Int. J. Heat and Mass Transfer*, Vol. 45, pp. 855-63.

Khanafer, K., Vafai, K. and Lightstone, M. (2003), "Buoyancy-driven heat transfer enhancement in a two dimensional enclosure utilizing nanofluids", *Int. J. Heat Mass Transfer*, Vol. 46, pp. 3639-53.

Koo, J. and Kleinstreuer, C. (2005), "Laminar nanofluid flow in microheat-sinks", *Int. J. Heat Mass Transfer*, Vol. 48, pp. 2652-61.

Lee, S., Choi, S.U.S., Li, S. and Eastman, J.A. (1999), "Measuring thermal conductivity of fluids containing oxide nanoparticles", *J. of Heat Transfer*, Vol. 121, pp. 280-9.

Liu, K.V., Choi, S.U.S. and Kasza, K.E. (1988), "Measurement of pressure drop and heat transfer in turbulent pipe flows of particulate slurries", Argonne National Laboratory Report, ANL-88.

Maiga, S.E., Nguyen, C.T., Galanis, N. and Roy, G. (2004), "Heat transfer behaviours of nanofluids in a uniformly heated tube", *Super Lattices and Microstructures*, Vol. 35 Nos 3-6, pp. 543-57.

Masuda, H., Ebata, A., Teramae, K. and Hishinuma, N. (1993), "Alteration of thermal conductivity and viscosity of liquid by dispersing ultra-fine particles (dispersions of (– Al_2O_3, SiO_2, and TiO_2 ultra-fine particles)", *Netsu Bussei (Japan)*, Vol. 4, pp. 227-33.

Maxwell, J.C. (1873), *Electricity and Magnetism*, Clarendon Press, Oxford.

Maxwell, J.C. (1904), *A Treatise on Electricity and Magnetism*, Oxford University Press, Cambridge.

Mori, Y., Futagami, K., Tokuda, S. and Nakamura, M. (1966), "Forced convective heat transfer in uniformly heated horizontal tubes, 1st report, experimental study on the effect of buoyancy", *Int. J. Heat Mass Transfer*, Vol. 9, pp. 453-63.

Nesreddine, H., Galanis, N. and Nguyen, C.T. (1997), "Variable-property effects in laminar aiding and opposing mixed convection of air in vertical tubes", *Numerical Heat Transfer; Part A*, Vol. 31 No. 1, pp. 53-69.

Pak, B.C. and Cho, Y.I. (1998), "Hydrodynamic and heat transfer study of dispersed fluids with submicron metallic oxide particles", *Exp. Heat Transfer*, Vol. 11 No. 2, pp. 151-70.

Patankar, S.V., Ramadhyani, S. and Sparrow, E.M. (1978), "Effect of circumferentially non-uniform heating on laminar combined convection in a horizontal tube", *J. Heat Transfer, Trans, ASME, Ser. C*, Vol. 100, pp. 63-70.

Petukhov, B.S., Polyakov, A.F. and Strigin, B.S. (1969), "Heat transfer in tubes with viscous-gravity flow", *Heat Transfer-Soviet Research*, Vol. 1, pp. 24-31.

Putra, N., Roetzel, W. and Das, S.K. (2003), "Natural convection of nano fluids", *J. Heat Mass Transfer*, Vol. 39, pp. 775-84.

Roy, G., Nguyen, C.T. and Lajoie, P.R. (2004), "Numerical investigation of laminar flow and heat transfer in a radial flow cooling system with the use of nanofluids", *Supper Lattices and Microstructure*, Vol. 35, pp. 497-511.

Siegwarth, D.P. and Hanratty, T.J. (1970), "Computational and experimental study of the effect of secondary flow on the temperature field and primary flow in a horizontal tube", *Int. J. Heat Mass Transfer*, Vol. 13, pp. 27-42.

Wang, X., Xu, X. and Choi, S.U.S. (1999), "Thermal conductivity of nanoparticle-fluid mixture", *J. Thermophys. Heat Transfer*, Vol. 13 No. 4, pp. 474-80.

Xuan, Y.M. and Li, Q. (2000), "Heat transfer enhancement of nanofluids", *Int. J. Heat and Fluid Flow*, Vol. 21, pp. 58-64.

Xuan, Y.M. and Li, Q. (2003), "Investigation on convective heat transfer and flow features of nanofluids", *J. Heat Transfer*, Vol. 125, pp. 151-5.

Xuan, Y.M. and Roetzel, W. (2000), "Conceptions for heat transfer correlation of nanofluids", *Int. J. Heat Mass Transfer*, Vol. 43 No. 19, pp. 3701-7.

Xuan, Y.M., Li, Q. and Hu, W. (2004), "Aggregation structure and thermal conducting of nanofluids", *AIChE J*, Vol. 49 No. 4, pp. 1038-43.

Xue, Q.Z. (2003), "Model for effective thermal conductivity of nanofluids", *Physics Letter A*, Vol. 307 Nos 5/6, pp. 313-7.

Yang, Y., Zhang, Z.G., Grulke, E.A., Anderson, W.B. and Wu, G. (2005), "Heat transfer properties of nanoparticle-in-fluid dispersions (nanofluids) in laminar flow", *Int. J. Heat and Mass Transfer*, Vol. 48 No. 6, pp. 1106-16.

Zhang, C. (1992), "Mixed convection inside horizontal tubes with nominally uniform heat flux", *AIChE Symposium Series*, Vol. 88 No. 288, pp. 212-9.

Corresponding author
A. Behzadmehr can be contacted at: behzadmehr@hamoon.usb.ac.ir